Electrical Relaxations in Mixtures of Lithium Chloride and Glycerol[1)]

F. Scott HOWELL,* Cornelius T. MOYNIHAN,† and Pedro B. MACEDO††
Department of Chemistry, Faculty of Science and Technology, Sophia University, Kioicho 7-1, Chiyoda-ku, Tokyo 102
††*Vitreous State Laboratory, Department of Chemical Engineering and Materials Science, The Catholic University of America, Washington, D.C. 20064, U.S.A.*
(Received July 22, 1983)

The dielectric constant ε' and the electrical conductivity σ were measured as a function of frequency (0.1—2 MHz) and temperature for an electrolyte-polar solvent system: lithium chloride in glycerol. Mole fractions of LiCl were 0, 1, 2, 5, 10, 20, and 33.3%. Data were analysed in terms of an inverse complex permittivity (electrical modulus). At lower mole fractions, two separate modulus relaxations were observed, one due to the ionic diffusion and the other to the dipole reorientation. These two relaxation processes converged with increasing LiCl mole fraction and were not distinguishable at 20%. The moduli isotherms at 33.3% were characteristic of a fused salt. Average relaxation times and distributions for both processes were determined by computer fits to a Gaussian distribution in the logarithms of these times. Their temperature and mole fraction dependences are discussed. The conductivity relaxations became slightly broader than single at 10%; this shows the influence of the charge concentration on the structural relaxation process.

Numerous studies have been conducted on dielectric relaxation in solutions of electrolytes in polar solvents. Some of these have been limited because the frequency, temperature, and/or concentration ranges studied were narrow. We report here a study of electrical relaxations in mixtures of LiCl in glycerol[2)] covering the 0—33.3 mol% LiCl range, i.e., from the dilute solution to the solvated melt where the number of solvent molecules is sufficient to fill more than the first solvation sphere of the ions.[3)] These solutions are highly viscous and supercool readily, so a wide range of temperature can be investigated over a wide frequency range in which accurate complex permittivity measurements can be made by conventional audio bridge techniques. The purpose of this work was to determine as a function of composition the relative contributions of ionic transport and reorientation of polar solvent molecules to the electric field relaxation in the mixture.

Experimental

Materials. A stock solution of lithium chloride in glycerol, containing nominally 33.3 mol% LiCl, was prepared by weight from Fisher Certified Reagent grade LiCl and Fisher Reagent grade glycerol. The salt was placed in a flask and dried to constant weight in an oven at 160 °C before the glycerol was added. The mixture, in a tightly-capped flask, was then heated and stirred on a hot-plate magnetic stirrer to bring the salt into solution. This 33.3% solution was too viscous to flow readily at room temperature and could be poured only when hot. The lower mole fraction mixtures (approximately 20, 10, 5, 2, and 1%) were formed by dilution of the 33.3 mol% mixture with glycerol. The pure glycerol and all mixtures were stored in tightly-capped flasks in a dessicator.

All the solutions were analyzed by titration of chlorine ions with a silver nitrate solution using the absorption indicator method. The density measurements for glycerol agreed with Bosart and Snoddy's results.[4)] The kinematic viscosity of the pure glycerol, measured at (20.0±0.1) °C with a factory-calibrated Cannon-Fenske capillary viscometer, was 0.0014 $m^2 s^{-1}$ (14 St), which corresponds to a glycerol–water solution of 0.998 mass fraction.[5)]

Apparatus and Procedures. Glass transition temperatures for glycerol and the mixtures were measured on a Perkin-Elmer differential scanning calorimeter (DSC-1B) at a heating rate of twenty degrees per minute. T_g was taken as the extrapolated point at which the heat capacity curve begins to rise rapidly.[6)]

The cell was described previously.[7,8)] Its vacuum capacitance was measured before each sample was poured in. This C_0 value changed slightly whenever the cell was disassembled for cleaning and then reassembled; it ranged from 0.81 to 0.90 pF.

Measurements of the equivalent parallel capacitance C and the conductance G were carried out over the frequency range 0.1 Hz to 2 MHz. We used a modified Cole-Berberian[9)] bridge (0.1 Hz to 500 Hz), a General Radio 1615A bridge (500 Hz to 100 kHz), and a Wayne-Kerr B601 bridge (15 kHz to 2 MHz). Electronic frequency counters (Hewlett-Packard 522B or 3734-A) were used to assure frequency accuracy wthin 0.2%.

The LiCl–glycerol mixtures were thermostated in a Tenney Jr. Environmental Chamber. The temperature range from −85 to −20 °C was sufficient to cover the relaxations studied. Chamber temperatures were determined with an accuracy of 0.1 °C by calibrated copper-constantin thermocouples located at the cell.

Densities of three of the mixtures were measured at 0 °C and at room temperature with a dilatometer.

Results and Discussion

Solution Properties. Table 1 compares the result of the composition analysis with the mixture compositions calculated from the reagent masses used. The densities and the glass transition temperatures are also listed.

The T_g measured for glycerol (192.8 K) does not agree with the value reported by Matheson *et al.* ((186.0 ±2) K).[10)] They used a DTA technique with a scanning rate of two degrees per minute. The discrepancy may be resolved by the difference in scanning rates (20 *vs.* 2 K min^{-1}), by uncertainties in our DSC temperature scale, or by differences in the water content of the glycerol samples studied.

† Present address: Rensselaer Polytechnic Institute, Troy, New York 12181, U.S.A.

TABLE 1. LiCl IN GLYCEROL: ANALYTICAL RESULTS

Nominal[a] content LiCl/mol%	Nominal content LiCl/wt%	Analysed content LiCl/wt%	Density[b] g cm^{-3}	T_g[c] K
Glycerol	0		1.275	192.8
1	0.462	0.474		191.9
2	0.931	0.926		
5	2.364	2.378		195.6
10	4.87	4.86	1.299	200.1
20	10.32	10.29	1.323	208.6
33.3	18.71	18.68		229.5

a) Calculated by assuming that the glycerol was 100% pure. b) At 0 °C; the changes in density per degree were -6.0×10^{-4} g cm^{-3} K^{-1}. c) Uncertainty: ±2 K.

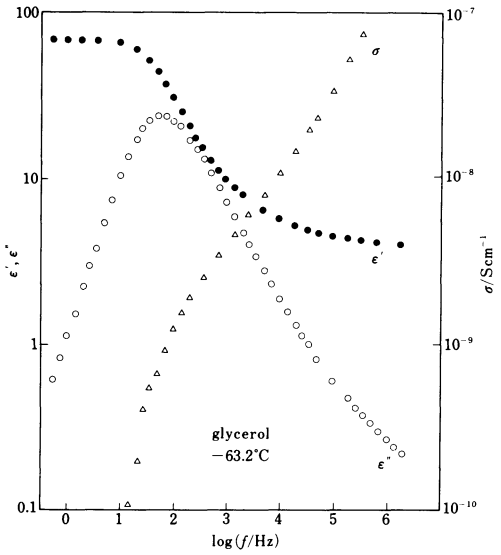

Fig. 1. Frequency dependence of conductivity △ and complex permittivity, ε': ● and ε'' :○, for glycerol at −63.2 °C. Left-side scale for permittivity, right-side scale for conductivity.

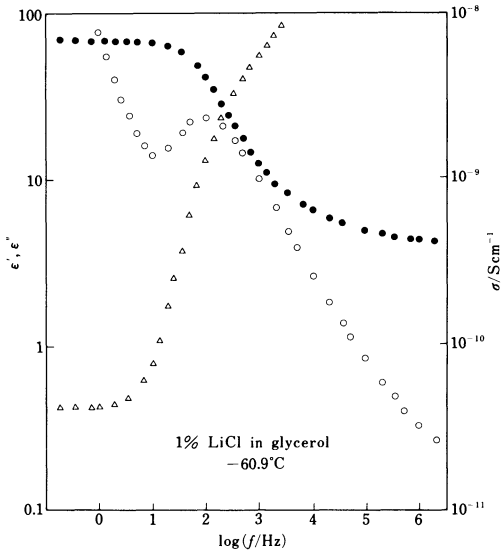

Fig. 2. Frequency dependence of conductivity and complex permittivity for 1 mol% LiCl in glycerol at −60.9 °C. Symbols and scales in Fig. 1.

Conductivities σ and dielectric constants (real parts of the complex relative permittivities) ε' were calculated from the experimental parallel G and C values *via* these equations:

$$\sigma = \varepsilon_0 G/C_0, \quad \varepsilon' = C/C_0, \tag{1}$$

where ε_0 is the permittivity of free space. Complete tables of σ and ε' values as functions of temperature and frequency are available.[1] In Figs. 1—4, experimental values of σ, ε', and $\varepsilon''=G/2\pi fC_0$ are plotted as a function of the logarithm of the measurement frequency f for glycerol and three mole fractions of LiCl in glycerol. At the temperatures selected, the complete relaxation could be seen within the experimentally available frequency range.

At low frequencies, the conductivity of the salt-glycerol mixtures becomes frequency-independent at the value σ_0. For glycerol this value is apparently much lower than the values available in these experiments.

The real part of the complex permittivity exhibits a frequency-independent shoulder (typically one decade wide) at low frequencies. This value is designated as ε_g

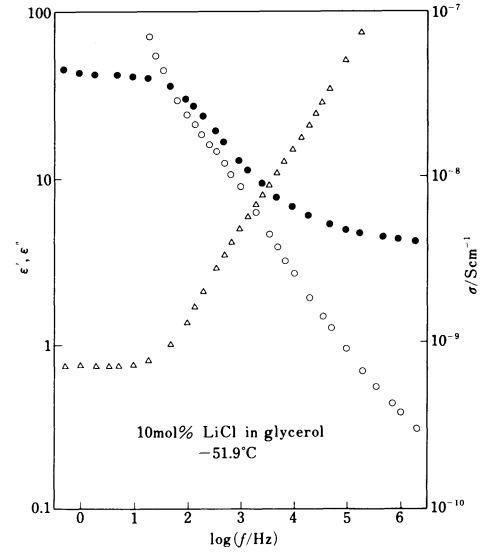

Fig. 3. Frequency dependence of conductivity and complex permittivity for 10 mol% LiCl in glycerol at −51.9 °C. Symbols and scales in Fig. 1.

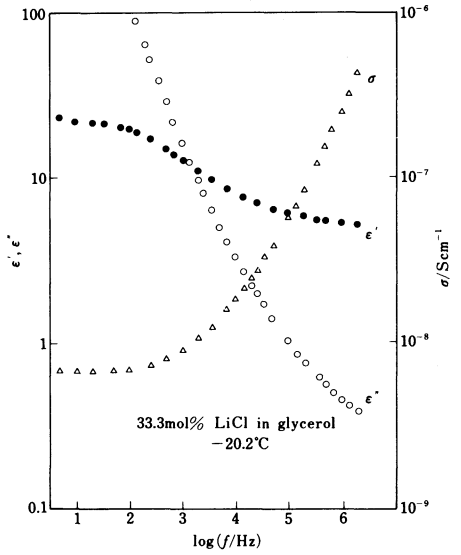

Fig. 4. Frequency dependence of conductivity and complex permittivity for 33.3 mol% LiCl in glycerol at −20.2 °C. Symbols and scales in Fig. 1.

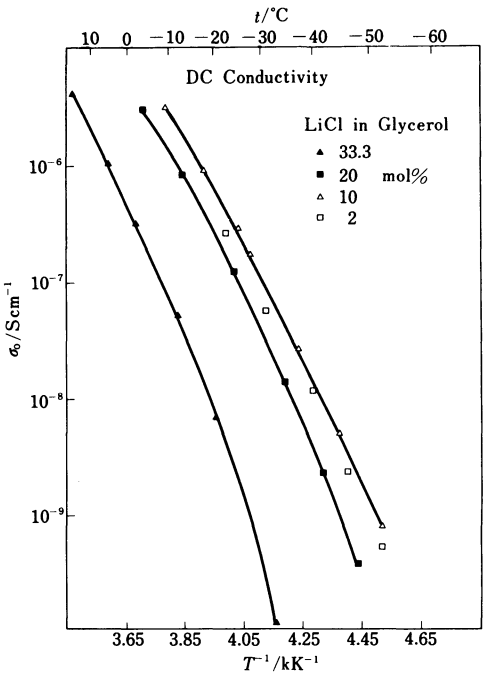

Fig. 5. Arrhenius plots of d.c. conductivity: 2, 10, 20, and 33.3 mol% LiCl in glycerol.

for glycerol and as ε_{LCg} for the salt-glycerol mixtures. The very rapid rise in ε' at still lower frequencies (beginning, for example, in Fig. 3 below 1 Hz and in Fig. 4 below 10 Hz) is due to electrode polarization and related sample-electrode interface effects which have been dealt with extensively in earlier papers.[7,11,12] These demonstrate that the frequency dependences of σ and ε' at frequencies higher than the frequency at which electrode-related effects are seen can be associated with the Li^+ ionic conductivity mechanism and with the glycerol dipole dielectric relaxation.

Figure 5 shows Arrhenius plots of the d.c. conductivity for the 2, 10, 20, and 33.3 mol% mixtures of LiCl. The 1% data fell slightly below the 2% points. The 5% data almost overlapped the line connecting the 10% points; the latter show a slightly higher activation energy. At a given temperature, the magnitudes of the d.c. conductivities occur in the following order: 33.3%≪20%≅1%<2%<5%≅10%.

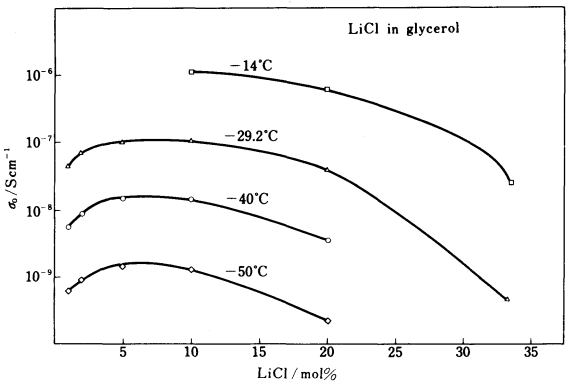

Fig. 6. Mole fraction dependence of d.c. conductivity for mixtures of LiCl in glycerol at various temperatures.

Figure 6 shows the d.c. conductivity as a function of mole fraction for various temperatures. A maximum in isothermal conductivity is seen between 5% and 10% mole fraction of LiCl. A similar maximum was reported by Bressel[13] for aqueous LiCl solutions and by Kartzmark *et al.*[14] for aqueous $LiNO_3$ solutions. The values of the molar conductivity, $\Lambda = \sigma_0/c$, where c is the amount-of-substance concentration, decrease monotonically with increasing mole fraction of LiCl and do not exhibit a minimum.

This maximum found in σ_0 can be explained by the mole fraction dependences of the different components of the conductivity. The value of the conductivity is given by $\sigma_0 = \sum N_i z_i \mu_i$, where N_i is the number of i-type ions per unit volume, z_i is the charge number of the ith ion, and μ_i is the electric mobility of the ith ion. N_i increases with increasing mole fractions of salt ions, but these additional ions introduce stronger electrical forces into the mixture and increase the viscosity and internal pressure. The total ionic diffusion mobility μ_i is inversely proportional to the average dielectric relaxation time, which is approximately the time for the mixture's local structure to break up. The ions will move as soon as the solvent structure opens to allow diffusive motion. This average dielectric relaxation time, in turn, is proportional to viscosity, by Debye's relation and McDuffie's results.[15] Thus the maximum found in σ_0 is due to the fact that the ionic electrical mobilities decrease much faster with increasing mole fraction of salt than the number of ions per unit volume increases.

Bartoli *et al.*[2] suggested that ion-pairing, which would decrease the N_i contribution to σ_0 at higher mole fractions, was responsible for the leveling out of σ_0 as a function of mole fraction. But this proposal neglects the mole fraction dependence of the ionic mobilities and does not easily explain the sharp decrease in σ_0 beyond 10 mol%. Nor is other evidence for ion-

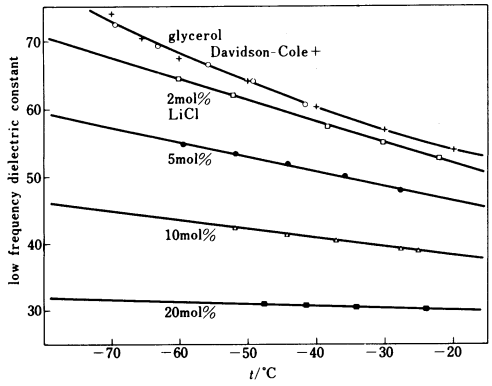

Fig. 7. Temperaure dependence of the low frequency dielectric constant for mixtures of LiCl in glycerol and for glycerol.

pairing available.

Figure 7 shows the low frequency limit of the real part of the complex permittivity as a function of temperature for glycerol and four mole fractions of salt in glycerol. The glycerol data of Davidson and Cole are included in the figure; the agreement is excellent.[16]

Within experimental error, the ε_{LCg} values for the 1% mole fraction were the same or slightly higher than the ε_g values and so have been omitted from Fig. 7.

The decrease of ε_g and ε_{LCg} with increasing temperature is due to the increasing thermal energy in the liquid mixture; this increased energy opposes the forces due to the external field, which tend to align the glycerol dipoles. Pottel has reported a similar temperature dependence for 1 mol dm^{-3} aqueous solutions of divalent sulfate salts.[17]

Modulus Data. Figures 8 and 9 show the low frequency dependences of the real and imaginary parts of the inverse complex relative permittivity, or complex electrical modulus, for each mole fraction of LiCl in glycerol at a selected temperature. The temperatures were chosen so that the entire electrical relaxation fell with the frequency ranges of the modified Cole-Berberian and General Radio bridges. In these figures, some data sets at higher mole fractions were shifted along the horizontal frequency axis by the number of decades indicated in the legend. At the lowest frequencies both M' and M'' decrease to zero. The zero lines are stepped up by the vertical scale shifts indicated in the legends. The 2% data for M'' at frequencies above 100 Hz overlap the 1% data and are omitted from the figure for convenience. Higher mole fraction data sets of M'' also have high frequency points which would appear on the figure beyond the peak; these have also been omitted.

Figure 10 shows the real and imaginary parts of the complex modulus for pure glycerol at −63.2 °C. Notice that the low frequency value of M' levels out at a non-zero value.

The complex modulus M^* is a function of angular frequency:

$$M^* = M' + iM'' = (\varepsilon^*)^{-1} = \varepsilon'/(\varepsilon'^2+\varepsilon''^2) + i\varepsilon''/(\varepsilon'^2+\varepsilon''^2). \quad (2)$$

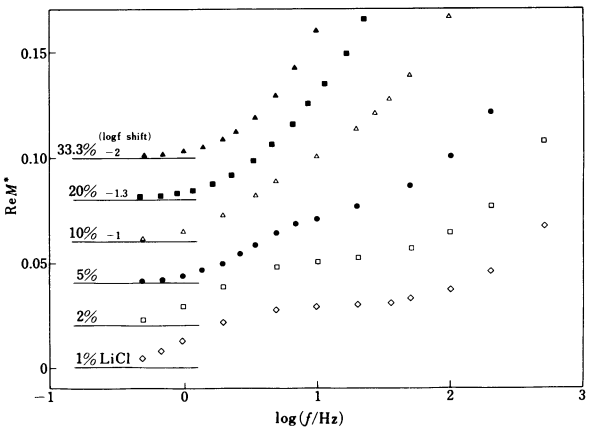

Fig. 8. Low frequency dependence of the real part of the complex modulus (M') of various mole fractions of LiCl in glycerol at typical temperatures. Vertical scale is labeled for 1 mol% data and should be stepped by 0.02 for each higher mole fraction. Horizontal scale is correct for 1, 2, and 5 mol% data; higher mole fraction data are shifted left as noted to avoid data overlap. Temperatures: 1 mol%, −60.9 °C; 2 mol%, −60.1 °C; 5 mol%, −51.8 °C; 10 mol%, −51.9 °C, frequency shifted by one decade; 20 mol%, −41.6 °C, frequency shifted by 1.3 decades; 33.3 mol%, −20.2 °C, frequency shifted by 2 decades.

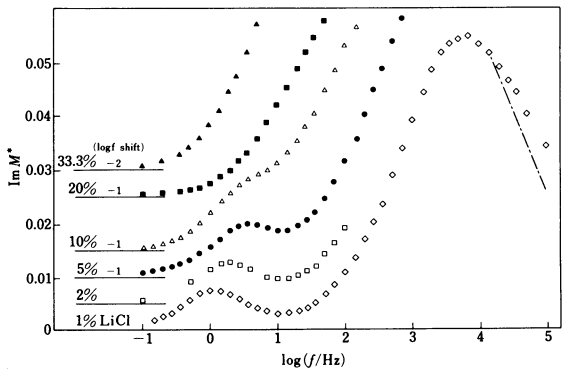

Fig. 9. Low frequency dependence of the imaginary part of the complex modulus (M'') of various mole fractions of LiCl in glycerol at typical temperatures, as listed in caption for Fig. 8. Vertical scale is labeled for 1 mol% data and should be stepped by 0.005 each for 2, 5, and 10 mol% data, by 0.01 for 20 mol% data, and again by 0.005 for 33.3 mol% data. Horizontal scale is correct for 1 and 2 mol% data; it should be shifted left by one decade for 5, 10, and 20 mol% data and by two decades for the 33.3 mol% data.

This formalism was first suggested in 1967 by McCrum *et al.*[18] and has been employed to describe electrical relaxations by analogy with the well-known compressional and shear moduli for viscoelastic flow.[11] The complex electrical modulus has been helpfully explained in terms of the more usual admittance, impedance, and permittivity formalisms by Hodge *et al.*[19] The mathematics of this M^* formalism has been developed in several reports.[7,8,12,19-21] The present case, in which a conducting dielectric

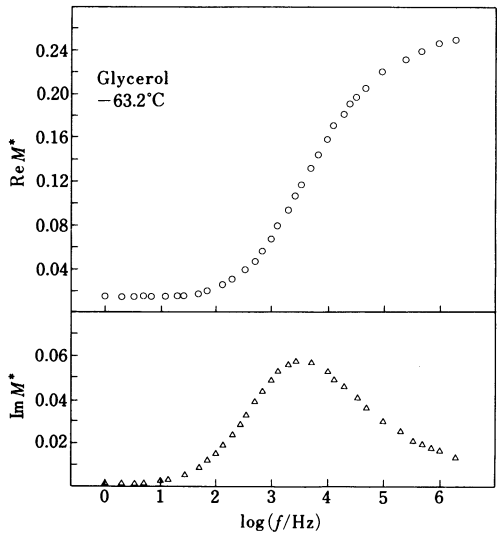

Fig. 10. Frequency dependence of the real (M') and imaginary (M'') parts of the complex modulus of glycerol at −63.2 °C.

undergoes a relaxation involving molecular mechanisms which do not contribute to the long-range conduction process, has been discussed in detail (see Eq. 15 in Refs. 7 and 21).

The complex modulus can be decomposed into two additive terms, which represent the conductivity relaxation (at lower frequencies) and the dielectric relaxation (at higher ones). If both these relaxations occurred at single relaxation times, the complex modulus equation would be

$$M^*(\omega) = M_s i\omega\tau_\sigma/(1+i\omega\tau_\sigma) + (M_\infty - M_s)i\omega\tau_D/(1+i\omega\tau_D). \quad (3)$$

Here M_s is the reciprocal of ε_s, the frequency-independent value of the dielectric constant at low frequency; M_∞ is the reciprocal of the high frequency value, ε_∞. τ_σ is the conductivity relaxation time. τ_D is the dielectric relaxation time at constant displacement vector and is related to the conventional dielectric relaxation time for constant electric field, τ_E, by $\tau_D=(M_s/M_\infty)\tau_E$.

One or both of the terms in Eq. 3 may need to be modified to allow for a distribution of relaxation times. In this work a log gaussian distribution of times[22-23] was used to generate best-fit curves to the M^* data at each temperature and concentration.

$$M^* = M_s\int_{-\infty}^{\infty} g_\sigma\left(\ln\frac{\tau_\sigma}{\tau'_\sigma}\right)\left[\frac{(\omega\tau_\sigma)^2+i\omega\tau_\sigma}{1+(\omega\tau_\sigma)^2}\right] d\ln\frac{\tau_\sigma}{\tau'_\sigma} + (M_\infty - M_s)\int_{-\infty}^{\infty} g_D\left(\ln\frac{\tau_D}{\tau'_D}\right)\left[\frac{(\omega\tau_D)^2+i\omega\tau_D}{1+(\omega\tau_D)^2}\right] \times d\ln\frac{\tau_D}{\tau'_D}. \quad (4)$$

The log gaussian distribution functions are the subscripted g's:

$$g_\sigma(\ln\tau_\sigma/\tau'_\sigma) = b_\sigma(\pi)^{-1/2}\exp(-b_\sigma^2\ln^2(\tau_\sigma/\tau'_\sigma)),$$
$$g_D(\ln\tau_D/\tau'_D) = b_D(\pi)^{-1/2}\exp(-b_D^2\ln^2(\tau_D/\tau'_D)). \quad (5)$$

Table 2. Gaussian fit parameters for glycerol

Temp °C	M_s	$M_\infty - M_s$	b_D	τ'_D μs
−41.7	0.0166	0.210	0.442	0.216
−49.1	0.0157	0.205	0.446	1.21
−55.8	0.0151	0.206	0.425	6.17
−63.2	0.0145	0.205	0.414	43.9
−69.4	0.0138	0.203	0.403	527.
−77.7	0.0132[a)]	0.201	0.396	22800

Standard deviations: 0.0002—0.00057. a) Estimated.

The primed *tau*'s are the most probable relaxation times for the respective distribution functions; the b values are inversely proportional to the widths of the distributions. A b value greater than 2.5 is considered equivalent to a delta function distribution, *i.e.* a single relaxation time. Fit parameters obtained at each temperature and concentration are given in Tables 2—5.

The M' data sets for glycerol level out at the expected non-zero $M_s=1/\varepsilon_s$ values at low frequencies. The fits shown in Table 2 were performed for data up to the peak in the M'' values.

For the dilute and moderately concentrated mixtures (1, 2, 5, 10 mol%), each conductivity and dielectric wave (in M') and peak (in M'') was fit separately to a log gaussian distribution. If sufficient data were available to show both peaks, a six-parameter function, the sum of two log gaussian distributions, was fit to the entire spectrum up to the top of the dielectric peak; this procedure reproduces Eq. 4. The 20 mol% data fits are discussed below. The 33.3 mol% data were fit to one broad log gaussian distribution; Table 5 shows the results.

For all cases, the data at frequencies beyond the maximum value of M'' were excluded when the least-squares fit was performed. No attempt was made to introduce a low, broad function centered a decade or so higher in frequency than the M'' maximum, a procedure which would probably have reproduced the high frequency shape of the data more adequately than the one we used. The high-frequency asymmetry in the M^* data which other authors[24] and ourselves[8,21] have reported was thus ignored. The generated fits fall inside the data points for frequencies beyond the dielectric M'' peak, as the dotted line for the 1 mol% data in Fig. 9 shows. All fits have an overall accuracy of about 3%; as might be expected, the fit is usually worst in the M'' valley between the conductivity peak and the dielectric peak.

The fit reported in Table 4 for the 20 mol% data was not acceptable. We believe that the conduction and the dipole reorientation processes contribute almost equally to the observed spectra. Extrapolation of the ratios of the average times (see below) as a function of concentration to the 20 mol% case indicated that the two peaks would be within a factor of ten in center frequencies. The six-parameter sum of two log gaussian distributions, however, was unable to separate the two presumed processes: the central

times could not be well-specified. Thus the fits shown in Table 4 are from a log gaussian distribution using three parameters which fortunately converged. This fit was in error by 100% for the data in the lowest decade of frequency, but it did match the data near the M'' maximum sufficiently closely for the fit program to converge.

Average Times. The average relaxation times

Table 3. Gaussian fit parameters for 1—10 mol% LiCl in glycerol

Temp °C	Conductivity fit M_s	b_σ	τ'_σ ms	Dielectric fit $M_\infty - M_s$	b_D	τ'_D μs	Ratio of average times
			— 1 mol% —				
−21.2	0.0189	1.90	0.0258				
−28.7	0.0180	1.80	0.0969				
−36.8	0.0165	single	0.495	0.204	0.433	0.0965	1432
−46.6	0.0157	single	4.16	0.194	0.441	0.812	1425
−52.9	0.0149	single	20.7	0.201	0.412	3.57	1327
−60.9	0.0144	single	140.	0.196	0.411	25.8	1239
−66.2	0.014[a]			0.192	0.403	260.	
−74.8	0.014[a]			0.189	0.397	9580	
			— 2 mol% —				
−22.0	0.0196	2.38	0.0143				
−30.3	0.0192	2.17	0.0748				
−38.5	0.0184	2.20	0.377				
−45.8	0.0176	2.41	1.96				
−52.1	0.0159	single	10.2	0.211	0.401	3.48	618
−60.1	0.0154	single	93.0	0.202	0.402	36.9	538
−66.9	0.015[a]			0.203	0.391	392.	
−75.3	0.015[a]			0.195	0.397	16200	
			— 5 mol% —				
−21.0	0.0245	1.33	0.00660				
−27.6	0.0241	1.19	0.0198				
−35.8	0.0188	single	0.122	0.209	0.416	0.147	196
−44.2	0.0181	single	0.777	0.207	0.404	0.930	181
−51.8	0.0171	single	5.33	0.208	0.388	6.27	162
−59.5	0.0162	2.18	50.3	0.206	0.376	66.3	136
−66.9	0.016[a]			0.202	0.374	806.	
−73.1	0.016[a]			0.196	0.386	19500	
			— 10 mol% —				
−37.1	0.0198	2.24	0.141	0.205	0.382	0.494	54
−44.4	0.0179	2.30	0.788	0.212	0.354	2.61	43
−51.9	0.0168	1.87	5.15	0.206	0.353	20.9	36
−60.6	0.0137	2.25	57.9	0.207	0.340	296.	24
−65.0	0.013[a]			0.196	0.358	3030	
−73.7	0.013[a]			0.188	0.406	247000	

a) Estimated.

Table 4. Compromise gaussian fit parameters for 20 mol% LiCl in glycerol

Temp °C	M_s	b	τ' μs
−13.3	0.191	0.290	0.0671
−24.1	0.196	0.289	0.441
−41.6	0.169	0.357	50.7
−47.8	0.162	0.396	402.
−55.4	0.153	0.466	7900

Standard deviations: 5.4×10^{-4}—1.2×10^{-3}.

Table 5. Gaussian fit parameters for 33.3 mol% LiCl in glycerol

Temp °C	M_s	b_σ	τ'_σ μs
−11.4	0.138	0.547	5.93
−20.3	0.142	0.566	45.1
−29.05	0.140	0.610	620
−33.8	0.144	0.609	2930
−39.6	0.145	0.633	34200

Standard deviations: $(4.8—6.6)\times10^{-4}$.

for each process can be calculated from the fit parameters. For a logarithmic gaussian distribution:[23]

$$\langle\tau\rangle = \tau' \exp(-1/4b^2). \quad (6)$$

The τ' and b are to be subscripted for either conductivity relaxation or dielectric relaxation at constant displacement vector (σ or D).

For the 20% data, the average time which this procedure generates is a compromise between $\langle\tau_\sigma\rangle$ and $\langle\tau_D\rangle$. A rough extrapolation of the ratios of the average times as a function of mole fraction indicated that the two times were within a factor of ten of each other when the LiCl mole fraction was about 20%.

The procedure of omitting from the fit the M^* data at frequencies beyond the dielectric M'' maximum had no significant effect on either of the average times calculated from the fit parameters.

Dielectric Times: Figure 11 shows the Arrhenius plots of the logarithms of the average dielectric relaxation times (at constant displacement vector) for glycerol and for the 1, 2, 5, and 10% LiCl mixtures with glycerol. At a given temperature, the increase in the magnitude of the logarithm of $\langle\tau_D\rangle$ from one to ten per cent was found to be linear with the mole fraction.

A wide distribution of dielectric relaxation times is observed. The cooperative aspects of the structural break-up are thus reflected in the dielectric behavior. The dielectric width parameter b_D decreases slightly with increasing concentration. Harris and O'Konski report a similar broadening for aqueous 1:1 electrolyte solutions.[25] They suggest that two processes are responsible for increasing the relaxation times of the polar solvent molecules. First, because more of the solvent molecules are bound in complexes with the cations at higher concentrations, there are fewer available to reorient freely with the applied electric field. Secondly, more of these free solvent molecules are in the second coordination shells of the solvated ions and are thus somewhat hindered in following the electric field.

At each concentration the dielectric width parameter b_D tends to increase with increasing temperature. This corresponds to a narrowing of the peak; Bartoli *et al.* found a similar narrowing in NaCl-glycerol mixtures.[2] As the temperature is increased, the amount of bonding in the liquid is lowered as the liquid structure becomes more randomized by the increased thermal energy of the individual molecules or complexes. The environmental relaxation model[26] had predicted such a temperature behavior of the width parameter associated with the structural rearrangement.

Conduction Times: Figure 12 shows the Arrhenius plots of the logarithms of the average conductivity relaxation times for all six mole fractions of LiCl in glycerol. $\langle\tau_\sigma\rangle$ decreases with increasing mole fraction for 1, 2, and 5 mol% LiCl. As the salt concentration in the sample increases, the conductivity increases; consequently, the electric field decays with a shorter time constant.

The 5 and 10 mol% values of $\langle\tau_\sigma\rangle$ are indistinguishable; the same line is used for both sets of data. These time values reflect the reversal in the concentration dependence of the d.c. conductivity in Fig. 6.

Distribution of Conduction Times: The dilute salt-glycerol mixtures show a single relaxation time for the conductivity relaxation at those temperatures at which sufficient data are available for a six-parameter sum of two log gaussian functions to be fit. When

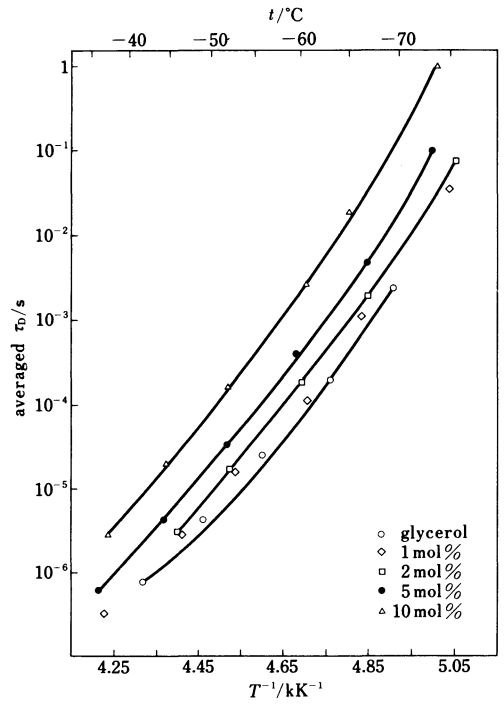

Fig. 11. Arrhenius plots of the average dielectric relaxation times at constant displacement vector for glycerol and for mixtures of 1, 2, 5, and 10 mol% LiCl in glycerol.

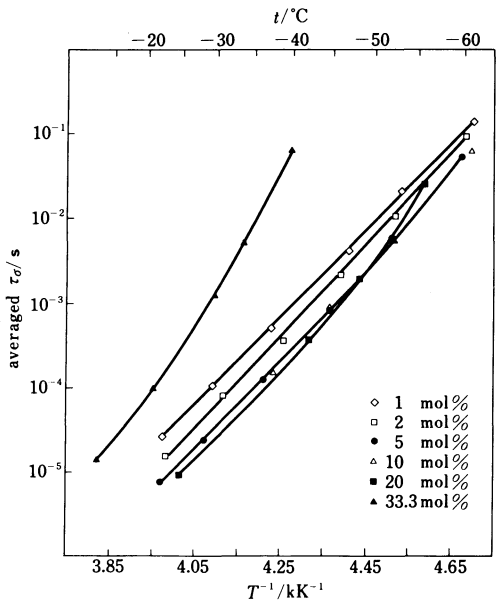

Fig. 12. Arrhenius plots of the average conductivity relaxation times for mixtures of 1, 2, 5, 10, 20, and 33.3 mol% LiCl in glycerol.

a 'single' relaxation is reported in the tables, b converged to a value greater than 2.5. Thus $\tau_\sigma' = \langle\tau_\sigma\rangle$. This result was confirmed by calculating the average relaxation times from the d.c. conductivity and the low-frequency frequency-independent value of ε', using $\langle\tau_\sigma\rangle = \varepsilon_0\varepsilon_s/\sigma_0$.[11] These independent calculations gave times which agreed with the fit values.

At the higher temperatures studied for these dilute salt-glycerol mixtures, only enough data was available to characterize the conductivity relaxation. Values of b_σ slightly lower than 2.5 were obtained, but these are an artifact of the fit procedure for the log gaussian function; this procedure included some of the data points beyond the M'' conductivity peak and thus some contribution from the beginnings of the dielectric relaxation. Single relaxation times were always achieved when both peaks were available for fitting.

Some structural considerations which could explain these results are given below. Besides these, the low concentration of charge carriers would give rise to long-range ionic conduction with little or no dispersion in ε' and σ at frequencies near the M'' conduction peak. This has been found to be the case in vitreous ionic conductors, specifically Phasil glass[27] and GeO_2,[28] as well as in ionically conducting single crystals which contain only a small concentration of charge carriers, such as NaCl crystals doped with divalent chlorides.[29]

The 10 mol% LiCl mixture shows a distribution of conduction relaxation times which is slightly broader than single. The average b_σ value is 2.17. At this moderate mole fraction, the number of charge carriers and the structural details of the glycerol reorientations are beginning to influence the conduction process. Part of the measured dispersion in ε' is thus due to the conductivity relaxation: this conclusion was impossible to draw using the complex permittivity data representation.[2]

Structural Consideration: This distribution of relaxation times which appears in the conduction modulus with increasing mole fraction of salt can be explained in terms of the interaction of the structural break-up process and the ionic diffusion process and by the increasingly cooperative character of the ionic conduction as the mole fraction of salt increases. We assume with Litovitz and McDuffie that the rate of an electrical relaxation is determined by the time in which a cooperative break-up occurs in the local structure of the liquid. Such a structural time would ordinarily be determined by an ultrasonic measurement, but it is reasonable to use the average dielectric relaxation time for constant displacement vector in place of the structural relaxation time for glycerol, since the ratio of the structural time and the usual dielectric relaxation time τ_E is only 1.5.[15,30]

If the characteristic time for structural relaxations is comparable to an electrical relaxation time, a distribution of electrical times is observed: this is the case for the dielectric relaxations reported here at all mole fractions. If, however, this structural time is much shorter than an electrical time, then the process will show a single electrical relaxation time, as is the case for the conductivity relaxations here at very low mole fractions.

When the mole fraction of ions is very low, the few ions present have to execute a large number of jumps in order to relax the electric field. If the ionic jump time is denoted as t_j, then we have $\tau_\sigma \gg t_j$ for the dilute cases. This also means that the field-biased ionic jumps are uncorrelated: the occurrence of a jump by a given ion does not bias the probability or direction of subsequent jumps by that ion or by other ions in its vicinity. At low concentrations, the details of the structural process are averaged out before the electric field decays, and thus the decay is seen as occurring with a single relaxation time.

When the mole fraction is increased to 10 mol%, however, it takes a much shorter time, that is, fewer jumps by a larger number of ions, before the field decays to zero. τ_σ becomes more comparable to t_j in this case. As the ionic concentration becomes higher, the average distance of ionic separation becomes smaller; thus the interionic coulombic interaction begins to become significant. The movement of an ion from one site to another will perturb the electrical potential in its vicinity; at a moderate mole fraction, other ions will be in the region of perturbed potential and their future motions will be biased. This cooperative motion of the ions will lead to a non-exponential decay function[24] and to dispersions in ε' and σ associated with long-range ionic migration.

Earlier reports[11,12] on alkali silicate glasses have followed Stevels,[31] Taylor,[32] and Isard[33] in suggesting that the dispersion in the complex permittivity would be accounted for by the lack of translational invariance of the free energy barriers impeding ionic diffusion in a vitreous quasi-lattice. These reports postulated that materials with a long-range lattice structure, such as ionic crystals, would have free energy barriers against ionic diffusion which would be regularly spaced and of equal height. For such equivalent lattice sites it was asserted that, on the average, the ions would spend the same duration of time at each site during the conduction process and that the long-range diffusion process would thus exhibit a single relaxation time. But recent experimental results for single crystals which contain a high concentration of charge carriers, $LiGaO_2$[34] and beta-alumina,[35] have shown a distribution of conductivity relaxation times when analysed in the complex modulus representation. These results underline the need in future theoretical work to pay more attention to the concentration of charge carriers. Not only a distribution of microscopic conductivities but also a moderate mole fraction of charge carriers, as in our 10 mol% LiCl mixture, can give rise to a distribution of conductivity relaxation times.

Jonscher[36] has advanced a model based on relaxation of screening charge about an ion following a jump, to account for the high frequency dispersion of the conductivity of dielectric materials. He had in mind producing an explanation only for the very high frequency losses due to localized motions, which are observed in all types of amorphous systems (insulators, ionic conductors, and electronic conductors), but his

model involves cooperative motion *via* interionic interactions and seems capable of expansion to the present system.

Higher Concentration Times: The 33.3 mol% average conduction times shown in Fig. 12 are much longer than the times for any of the other concentrations. This reflects the increase in viscosity and the sharp rise in the glass transition temperature for this concentration.

The 20 mol% average times are also displayed in Fig. 12 as if they were average conduction times, although we think that these apparent fit times are some compromise values between the dielectric reorientation time and the ionic conductivity time. The curvature in the Arrhenius plot is much different from that seen for the lower concentration data, especially at the lowest temperatures. The curve for the 20 mol% average times bends away from the slopes of the lower concentrations and towards the slope of the 33.3 mol% average conductivity times.

Distributions at Higher Concentrations: The 33.3 mol% data exhibit a wide conductivity relaxation. The magnitude of b_σ decreases by about 10% as the temperature increases. The modulus wave and peak broaden with increasing temperature in a way similar to the highly viscous liquid behavior of the glass-forming nitrate mixture studied earlier.[8] This similarity is another indication that the 33.3 mol% LiCl glycerol mixture should be considered a quasi-fused-salt.

The 20 mol% data show a wide distribution of relaxation times similar to that for the 33.3 mol% results. Over a temperature increase of about 40 K, the width parameter broadens from 0.466 to 0.290. This temperature dependence of the width parameter at least suggests the onset of fused salt behavior, even when it is remembered that the fit is only apparent (since the two times have moved so close together that the fit functions cannot separate them).

Ratios of Average Electrical Times: The ratio of the average conductivity relaxation time to the average dielectric relaxation time at constant displacement vector is given in Table 3, for those temperatures at which both relaxations could be adequately fit by the six-parameter sum of two gaussian functions. This ratio is a strong function of concentration, dropping from an average value of 1400 at 1 mol% LiCl to 580 at 2 mol%, 170 at 5 mol%, and about 40 at 10 mol%. This decrease in the $\langle\tau_\sigma\rangle/\langle\tau_D\rangle$ ratio with increasing concentration is due to the facts that $\langle\tau_\sigma\rangle$ decreases with concentration, remaining constant between 5 and 10 mol%, while $\langle\tau_D\rangle$ increases with concentration. The extrapolation of this dependence to 20 mol% LiCl yields a ratio of about six, while further extension to the 33.3 mol% case yields a value of less than one.

At a given concentration, an increase in temperature increases the magnitude of the ratio of electrical times. Over the temperature range −61 °C to −37 °C, the ratio increases by more than 15% for the 1 mol% mixture, while for the 10 mol% mixture the ratio more than doubles. Only when the ratio is less than 100 does the conductivity relaxation show a distribution of relaxation times.

The authors are grateful to M. Samanta and Dr. Regan Howard for their assistance with the chemical analyses and the DSC measurements. They are especially grateful to Dr. William Stamm for measuring the 2 mol% data. This research was partially supported by the United States Office of Naval Research. One of us (FSH) acknowledges with gratitude the Traineeship provided by the United States National Aeronautics and Space Administration.

References

1) F. S. Howell, Ph. D. Thesis, The Catholic University of America, Washington, D. C. (1972), Chap. 5; University Microfilms order number 72-22591.
2) F. J. Bartoli, J. N. Birch, N-H. Toan, and G. E. McDuffie, *J. Chem. Phys.*, **49**, 1916 (1968).
3) J. O'M. Bockris and A. K. N. Reddy, "Modern Electrochemistry," Plenum Press, New York (1974), pp. 76—80. The treatment is for water molecules.
4) L. W. Bosart and A. O. Snoddy, *Ind. Eng. Chem.*, **19**, 506 (1927).
5) M. L. Sheehy, *Ind. Eng. Chem.*, **24**, 1060 (1932).
6) C. A. Angell and E. J. Sare, *J. Chem. Phys.*, **52**, 1058 (1970).
7) J. H. Ambrus, C. T. Moynihan, and P. B. Macedo, *J. Phys. Chem.*, **76**, 3287 (1972).
8) F. S. Howell, R. A. Bose, P. B. Macedo, and C. T. Moynihan, *J. Phys. Chem.*, **78**, 639 (1974).
9) J. G. Berberian and R. H. Cole, *Rev. Sci. Instrum.*, **40**, 811 (1969).
10) M. R. Carpenter, D. B. Davies, and A. J. Matheson, *J. Chem. Phys.*, **46**, 2451 (1967).
11) P. B. Macedo, C. T. Moynihan, and R. Bose, *Phys. Chem. Glasses*, **13**, 171 (1972).
12) V. Provenzano, L. P. Boesch, V. Volterra, C. T. Moynihan, and P. B. Macedo, *J. Am. Ceram. Soc.*, **55**,492 (1972).
13) R. D. Bressel, Ph. D. Thesis, Purdue University, Lafayette, Indiana (1972); University Microfilms order number 72-21164. *Cf.* p. 102 and Fig. 42.
14) A. N. Campbell, G. H. Debus, and E. M. Kartzmark, *Can. J. Chem.*, **33**, 1508 (1955).
15) G. E. McDuffie, Jr., R. G. Quinn, and T. A. Litovitz, *J. Chem. Phys.*, **37**, 239 (1962); G. E. McDuffie, Jr., and T. A. Litovitz, *ibid.*, **37**, 1699 (1962); T. A. Litovitz and G. E. McDuffie, Jr., *ibid.*, **39**, 729 (1963).
16) D. W. Davidson and R. H. Cole, *J. Chem. Phys.*, **19**, 1484 (1951).
17) R. Pottel, "Chemical Physics of Ionic Solutions," ed by B. E. Conway and R. G. Barradas, Wiley, New York (1966), pp. 581—589.
18) N. G. McCrum, B. E. Read, and G. Williams, "Anelastic and Dielectric Effects in Polymeric Solids," Wiley, New York (1967), p. 110.
19) I. M. Hodge, M. D. Ingram, and A. R. West, *J. Electroanal. Chem. Interfacial Electrochem.*, **74**, 125 (1976).
20) C. T. Moynihan, R. D. Bressel, and C. A. Angell, *J. Chem. Phys.*, **55**, 4414 (1971).
21) C. T. Moynihan, L. P. Boesch, and N. L. Laberge, *Phys. Chem. Glasses*, **14**, 122 (1973).
22) T. A. Litovitz and C. M. Davis, "Physical Acoustics," ed by W. P. Mason, Academic Press, New York (1965), Vol. IIA, pp. 281—349.
23) W. A. Yager, *Physics*, **7**, 434 (1936).
24) G. Williams and D. C. Watts, *Trans. Faraday Soc.*, **66**, 80 (1970); G. Williams and P. J. Hains, *Faraday Symp. Chem. Soc.*, **6**, 14 (1972).

25) F. A. Harris and C. T. O'Konski, *J. Phys. Chem.*, **61**, 310 (1957).
26) H. Tweer, J. H. Simmons, and P. B. Macedo, *J. Chem. Phys.*, **54**, 1952 (1971).
27) C. T. Moynihan, J. H. Simmons, and P. B. Elterman, Glass Division Meeting, American Ceramic Society, Bedford, PA, October 14, 1976; Abstract in *Bull. Am. Ceram. Soc.*, **55**, 745 (1976).
28) H. Bohm, *J. Appl. Phys.*, **43**, 1103 (1972).
29) Y. Haven, *J. Chem. Phys.*, **21**, 171 (1953).
30) C. J. Montrose and T. A. Litovitz, "Neutron Inelastic Scattering," I. A. T. A., Vienna (1968), Vol. 1, pp. 623—637.
31) J. M. Stevels, "Handbuch der Physik," Springer-Verlag, Berlin (1957), Vol. 20, pp. 372—379.
32) H. E. Taylor, *J. Soc. Glass Technol.*, **41**, 350T (1957); **43**, 124T (1959).
33) J. O. Isard, *Proc. Inst. Elec. Engrs. (London)*, **109B**, Supplement 22, 440 (1962); *J. Non-Cryst. Solids*, **4**, 357 (1970).
34) R. J. Grant, I. M. Hodge, M. D. Ingram, and A. R. West, *J. Am. Ceram. Soc.*, **60**, 226 (1977).
35) R. J. Grant, I. M. Hodge, M. D. Ingram, and A. R. West, *Nature*, **226**, 42 (1977).
36) A. K. Jonscher, *Nature*, **253**, 717 (1975).